Positronium formation at Si surfaces

A. Kawasuso,[*] M. Maekawa, A. Miyashita, and K. Wada

National Institutes for Quantum and Radiological Science and Technology, 1233 Watanuki, Takasaki, Gunma 370-1292, Japan

T. Kaiwa and Y. Nagashima

Tokyo University of Science, 1-3, Kagurazaka, Shinjuku-ku, Tokyo 162-8601, Japan

Positronium formation at Si(111) and Si(001) surfaces has been investigated by changing the doping level systematically over the range 300–1000 K. The temperature dependence of the positronium fraction varied with the doping condition, and there were practically no differences between the two surface orientations. In heavily doped n-type Si ($n \gtrsim 10^{18}$ cm^{-3}), the positronium fraction (I_{Ps}) increased above 700 K and reached more than 95% at 1000 K. In undoped and lightly doped Si (n, $p \lesssim 10^{15}$ cm^{-3}), I_{Ps} decreased from 300 to 500 K and increased above 700 K. In heavily doped p-type Si ($p \gtrsim 10^{18}$ cm^{-3}), I_{Ps} increased in two steps: one at 500–600 K and one above 700 K. Overall, the positronium fraction increased with the amount of n-type doping. These phenomena were found to be dominated by two kinds of positronium with energies of 0.6–1.5 eV and 0.1–0.2 eV, which were attributed to the work-function mechanism and the surface-positron-mediated process, respectively, with contributions from conduction electrons. The positron work function was estimated to be positive. This agrees with first-principles calculation. The positive positron work function implies that the formation of excitonic electron-positron bound states begins in the bulk subsurface region and transits to the final positronium state in the vacuum.

I. INTRODUCTION

Positronium, which was predicted by Mohorovičić [1] and discovered by Deutsch [2], is the purely leptonic bound state composed of an electron and a positron. It is a very simple system, but it is still extensively investigated such as in the verification of the standard model of elementary particle physics [3] and quantum electrodynamics [4], the realization of high-T_C Bose-Einstein condensation (BEC) [5], and atomic physics [6]. In these studies, the generation of high-density positronium (e.g., 10^{18} cm^{-3} for positronium BEC) is an important issue. Solid surface is a medium to generate positronium. The positronium formation is sensitive to the surface condition such as adsorption. The angular and energy distributions of surface positronium reflect the momenta and energy levels of electrons in the surface layers of the solid. Hence, positronium may also be a unique probe to study the electronic state of the first surface layers [7,8]. It is, therefore, important to understand the generation processes of positronium at solid surfaces in detail.

At metal surfaces, positronium is generated via (i) the work-function mechanism, (ii) the surface positron state, and (iii) energetic positron scattering. Here, we focus on (i) and (ii). The positronium work function (Φ_{Ps}) is given as the summation of electron and positron work functions (ϕ_-, ϕ_+) and the energy gain due to positronium formation (-6.8 eV): $\Phi_{Ps} = \phi_- + \phi_+ - 6.8$ eV. If Φ_{Ps} is negative, spontaneous emission of positronium occurs with a maximum kinetic energy of $|\Phi_{Ps}|$.

Positrons are also trapped at the mirror potential formed at the surface-vacuum interface (surface positron state). In this case we define $E_S = \phi_- + E_B - 6.8$ eV, where E_B is the binding energy of the surface positron. Similar to (i), if E_S is negative, spontaneous positronium emission occurs with a maximum energy of $|E_S|$. Even in the case of positive E_S, positronium emission occurs as a thermal activation process with an energy of dozens of meV (thermal positronium).

For semiconductors, though surface positronium may be formed in ways similar to metals [9,10]. However, because of the band gap and the suppressed screening effect, dissimilar processes may also be expected.

In 2011, the group at the University of California, Riverside (UCR) found that at a Si(001) surface the positronium fraction increases with increasing temperature, while its kinetic energy exceeds the thermal region and hence it is not classified as conventional thermal positronium [11]. They also found enhanced positronium formation as the result of optical excitation [12]. Consequently, it was proposed that positronium is formed through an excitonic bound state between surface positrons and electrons (PsX state) [13,14]. Since only lightly doped Si(001) samples were used in the above work, further investigation that involves changing the doping level more systematically and using different surface orientations is required in order to explore the PsX hypothesis.

In this study, we measured the positronium fractions at Si(111) and Si(001) surfaces with different doping levels as a function of temperature. We also determined the positronium energy from the time-of-flight measurements. Through describing the positronium formation processes based on the experimental findings and first-principles calculation, we

———————
[*]kawasuso.atsuo@qst.go.jp

TABLE I. Sample characteristics.

	Dopant	Conduction type	Carrier density(cm^{-3})
Si(111)	Sb	n	1×10^{18}
	P	n	3×10^{15}
	Undoped	n	1×10^{12}
	B	p	1×10^{15}
	B	p	4×10^{18}
Si(001)	P	n	1×10^{19}
	Sb	n	1×10^{18}
	Undoped	n	1×10^{11}
	B	p	4×10^{18}

concluded that the excitonic bound state exists universally between positrons not only at the surface state but also in the bulk and conduction electrons.

II. EXPERIMENT

A. Procedure

The samples used in this study were Czochralsky-grown Si(111) and Si(001) wafers doped with phosphorus, antimony, or boron, and floating-zone-grown undoped Si(111) and Si(001) wafers. The sample thickness was 525 μm in all cases. The doping levels are listed in Table I. The samples were dipped into 50% hydrofluoric acid for 5 min and subsequently cleaned with ultrapure water without exposing them to air. From the hydrophobicity, the removal of the natural oxide layer and surface hydrogen termination were confirmed.

The samples were transferred into the vacuum chamber (base pressure: 8×10^{-7} Pa) equipped with a slow positron beam apparatus during 20 min in air. The beam apparatus is composed of a ^{22}Na source (1.1 GBq), a tungsten mesh moderator, and a magnetic transport system. The samples were injected with positrons with the energy of $E_+ = 200$ eV and annihilation γ-ray energy spectra were measured using a high-purity Ge detector as a function of temperature at $300 \sim 1000$ K ($27 \sim 727\,^\circ$C). In one spectrum, 5×10^5 counts were accumulated. Two-γ events created a sharp peak at 511 keV ($= m_0 c^2$, where m_0 is the electron rest mass and c is the light speed). Three-γ events gave rise to a continuous spectrum below 511 keV. The positronium fraction was determined using the 511 keV peak intensity denoted as P and the lower energy spectrum intensity denoted as R:

$$I_{\mathrm{Ps}} = \left[1 + \frac{P_{100\%}}{P_{0\%}} \frac{R_{100\%} - R}{R - R_{0\%}} \right]^{-1}, \qquad (1)$$

TABLE II. Calculated positron affinity (A_+), positronium work function (Φ_{Ps}), electron and positron work functions (ϕ_-, ϕ_+), surface dipole barrier (Δ), and surface positron binding energy (E_B) in eV.

Bulk calculation		Slab calculation				
A_+	Φ_{Ps}	Surface	ϕ_-	ϕ_+	Δ	E_B
-6.38	-0.42	(111)	$+4.56$	$+1.82$	$+10.86$	$+2.70$
		(001)	$+4.54$	$+1.84$	$+10.84$	$+2.41$
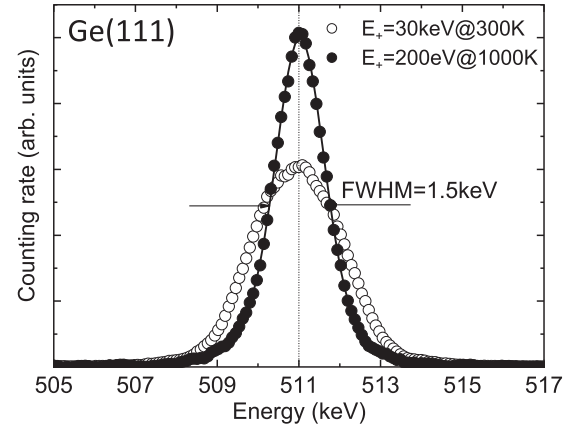
FIG. 1. Annihilation γ-ray spectra at 511 keV obtained for Ge(111) at 1000 and 300 K with positron energies of $E_+ = 200$ eV and $E_+ = 30$ keV, respectively. In the latter condition, positronium formation is negligible.

where the subscript denotes the 100(0)% positronium intensity determined from measurements of Ge(111) at 1000 K and mica at 300 K [15–17]. As shown in Fig. 1, a very sharp 511 keV peak is seen for the Ge sample at 1000 K and $E_+ = 200$ eV as compared to 300 K and $E_+ = 30$ keV, where positronium formation is negligible. The full width at half maximum is 1.5 keV. This is comparable to the detector resolution, suggesting the peak is arising from nearly 100 % (para) positronium.

The samples were also subjected to positronium time-of-flight measurements at the Slow Positron Facility of the High Energy Acceleration Research Organization in Japan [18]. Pulsed positrons generated by an electron linac were injected into the samples at $E_+ = 200$ eV. Positronium annihilation events were detected using scintillation-photomultiplier detectors located 40 and 120 mm upstream from the sample position. Positronium time-of-flight spectrum was acquired using the pulse signals from the linac and the annihilation γ rays.

In the preliminary measurements, after heating the samples to 1000 K, the positronium formation was observable. After cooling the samples to 300 K, the positronium fraction was found to decrease exponentially to approximately half in half a day. Whereas, when the samples were kept above ~ 348 K (75 $^\circ$C), the degradation of the positronium fraction was suppressed. After keeping the samples at 300 K for a long time, the temperature dependence obtained in the first run was no longer reproduced. These results show that the sample surfaces were contaminated during the transportation in air and even in the vacuum chamber with residual gases. During heating to 1000 K, surface contaminants and hydrogen atoms were considered to be desorbed together. Thus, in all the experiments, the positronium fraction was measured from 1000 to 300 K, and then again to 1000 K to confirm the absence of thermal hysteresis. After one cooling and heating run, the samples were replaced by new ones.

B. Results

Figure 2 shows the temperature dependence of the positronium fraction (I_{Ps}) obtained for all the samples. In the cooling
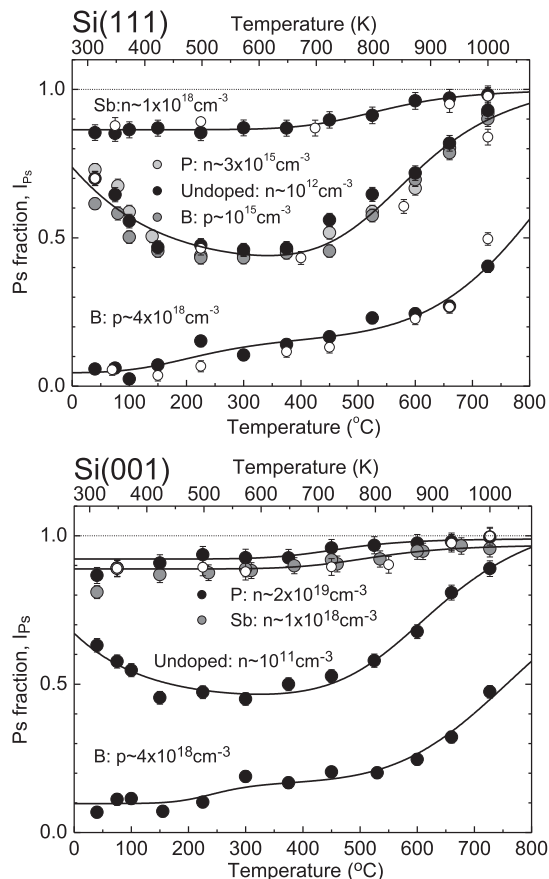
FIG. 2. Temperature dependences of positronium fraction obtained for the Si(111) and Si(001) samples with different doping conditions. Filled and open circles are obtained in the cooling and heating runs, respectively. Solid lines are the fitting curves using Eqs. (5)–(7).

FIG. 3. Positronium fraction obtained for the doped and undoped Si(111) samples at 373 K (100 °C) as a function of incident positron energy.

and heating runs, no thermal hysteresis is seen. The overall positronium fraction increases in the order of heavily doped p-type → undoped and lightly doped → heavily doped n-type. The increase of I_{Ps} from $n \sim 10^{18}$ to 10^{19} cm^{-3} is only small, as seen for the Si(001) sample. Several thermal processes are seen, which can be described as follows. In the heavily doped n-type samples, I_{Ps} increases above 700 K and reaches almost 100% at 1000 K. In the heavily doped p-type samples, I_{Ps} increases in two steps (i.e., at 500–600 K and above 700 K). In the undoped and lightly doped samples, I_{Ps} decreases from 300 to 500 K and then increases above 700 K. The increase of I_{Ps} above 700 K seems to be common for all the samples.

Thus, the amount of positronium and its temperature dependence strongly depends on the doping condition. There are no essential differences between Si(111) and Si(001) surfaces. Some of these features complement the results of the previous works [11–14], which mainly used lightly doped Si(001) samples.

Figure 3 shows the positronium fraction for the Si(111) samples at 373 K (100 °C) as functions of incident positron energy and mean positron implantation depth [19]. The results for the Si(001) samples were nearly the same. In the heavily doped p-type and undoped samples, only small amount

of positrons implanted in shallow regions participated in positronium formation. Whereas, in the heavily doped n-type sample, implanted positrons effectively returned to the surface giving rise to a large amount of positronium. The effective drift diffusion of positrons in n-type semiconductors has been known for a long time. It is explained as an effect of the electric field induced by the band bending near the surface [20,21].

Figure 4 shows the positronium time-of-flight spectra obtained for the heavily doped n-type, undoped, and heavily doped p-type Si(111) samples at different temperatures after subtracting the ortho-positronium lifetime backgrounds [$\propto \exp(-t/142)$ ns]. There are two characteristic components. One has a peak at $E_{Ps} \sim 0.6$ eV and threshold at $E_{Ps} \sim 1.5$ eV. The other has a peak at $E_{Ps} = 0.1$–0.2 eV. The energies of two kinds of positronium agree with those obtained by the UCR group for Si(001) and Si(111) surfaces [11–14]. Here, these components are termed type A ($E_{Ps} = 0.6$–1.5 eV) and type B ($E_{Ps} = 0.1$–0.2 eV). Apart from these components, no thermal positronium ($E_{Ps} \leqslant 90$ meV) is seen.

In the heavily doped n-type and undoped samples, type A positronium exists in the whole temperature range, while type B positronium appears at high temperatures. In the heavily doped p-type sample, type A positronium is nearly absent at 348 K and appears above 600 K. Type B positronium exists in the whole temperature range and increases above 700 K.

III. THEORETICAL CALCULATION

To interpret the experimental data quantitatively, two-component density functional theory (TC-DFT) calculations (conventional scheme) were carried out by using the ABINIT code [22] with the projector-augmented-wave method [23] within the generalized gradient approximation (GGA) [24]. The electron-positron correlation energy functional was based on the GGA method [25]. The valence electron configuration of the Si atom was assumed to be $2s^2 2p^6 3s^2 3p^2$. The bulk calculation was carried out using a primitive cell composed of two Si atoms with full structural optimization. The k-point sampling was $15 \times 15 \times 15$. The optimized lattice constant was $a = 5.47$ Å. The positronium work function was
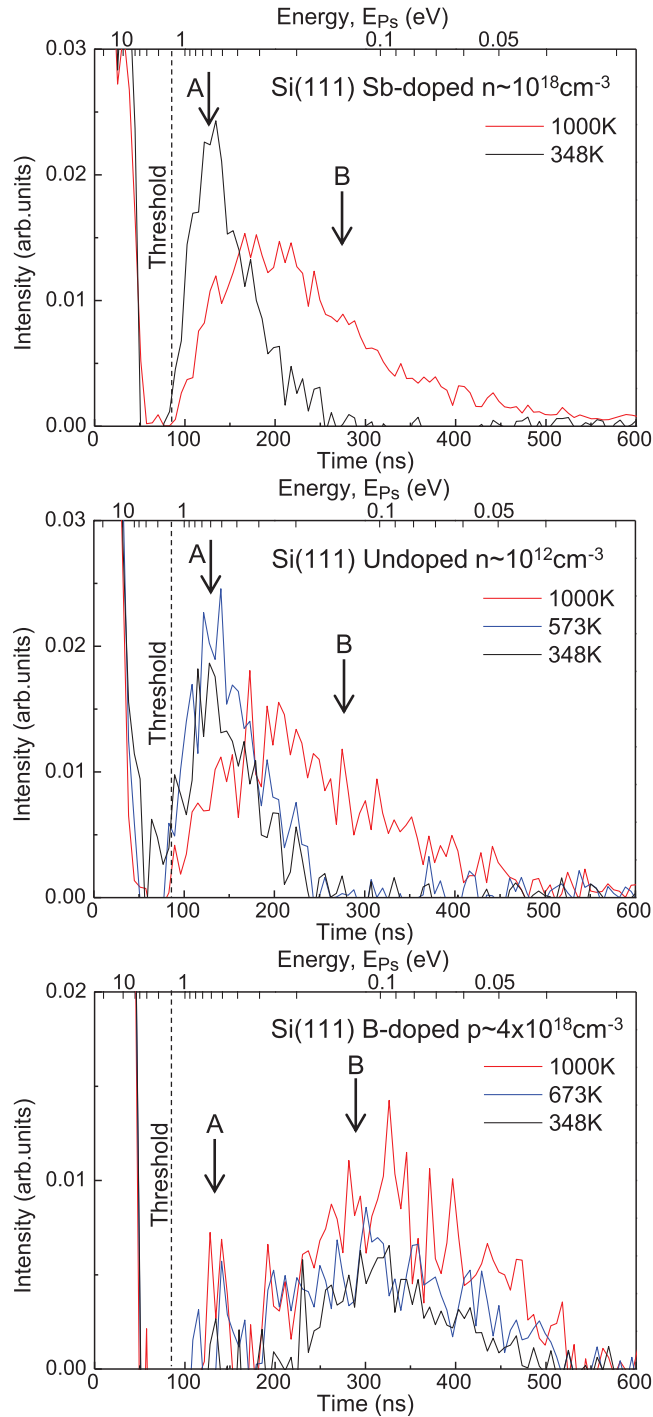
FIG. 4. Positronium time-of-flight (Ps-TOF) spectra obtained for the Si(111) samples for different doping conditions at the highest (1000 K), medium (573 and 673 K) and lower (373 and 348 K) temperatures. Vertical broken lines denote the threshold of the TOF spectra (~1.5 eV). Arrows denote the approximate peak positions of two types of Ps distinguished by their energies.

determined as

$$\Phi_{Ps} = -A_+ - 6.8 \text{ eV} = -(\mu_- + \mu_-) - 6.8 \text{ eV}, \quad (2)$$

where A_+ is the positron affinity and $\mu_\mp$ is the electron (positron) chemical potential measured from the crystal zero.

The positron work function and surface dipole barrier were determined, respectively, by

$$\phi_+ = -A_+ + \phi_- \quad \text{and} \quad \Delta = -A_+ + \mu_-. \quad (3)$$

For the calculations of electron work function and surface positron binding energy, Si(111) and Si(001) slab crystals composed, respectively, of 12 and 13 monolayers oriented in the surface normal direction with the primitive cell oriented in the surface parallel direction were constructed. The vacuum layer was initially assumed to be 20 Å. For the electron calculation, the k-point sampling was $9 \times 9 \times 1$. The (111) and (001) surfaces were assumed to be bulk truncated and dimer structures, respectively. To determine the positron surface state precisely, a corrugated mirror potential was implemented as the surface potential for positrons [26–28]. The contact point of image potential and electron-positron correlation potential (effective image plane) was determined in a way similar to the previous study [29]. Traditionally, the local-density approximation (LDA) electron-positron correlation potential is connected to the corrugated mirror potential. Here, the GGA electron-positron correlation potential was used since it gives better results in the evaluations of surface positron binding energy and annihilation lifetime as compared to the LDA potential [28,30]. For the positron calculation, only the Γ point was considered. Full structural optimization was also carried out.

Table II shows the results of the calculation. The positronium work function is in good agreement with that obtained by Kuriplach and Barbiellini [31]. The positron work function is positive for both (111) and (001) surfaces. The surface positron binding energies are in good agreement with those obtained by Fazleev *et al.* [29]. These results imply that the spontaneous emission of positronium occurs, there is no positron emission, and the surface positron state exists.

IV. DISCUSSION

Figure 5(a) shows the schematic representation of the temperature dependence of the positronium fraction for the three typical doping conditions shown in Fig. 2. As denoted by the arrow, the overall positronium fraction increases from heavily doped *p*-type to heavily doped *n*-type Si. There are three kinds of temperature dependence: (I) the process decreasing with temperature, which is seen only for undoped and lightly doped Si; (II) the process increasing with temperature, which is seen only for heavily doped *p*-type Si; and (III) the process increasing with temperature, which is seen for all the doping conditions.

Figure 5(b) shows the temperature ranges of type A and type B positronium. In undoped and lightly doped Si, and heavily doped *n*-type Si, type A positronium exists in the entire temperature range, while type B positronium appears only above 700 K. In heavily doped *p*-type Si, type A positronium appears only above 600 K, while type B positronium exists in the whole temperature range and increases above 700 K. The problem here is how to explain these experimental facts.

(a) Temperature dependence of Ps fraction

(b) Temperature ranges of two types of Ps
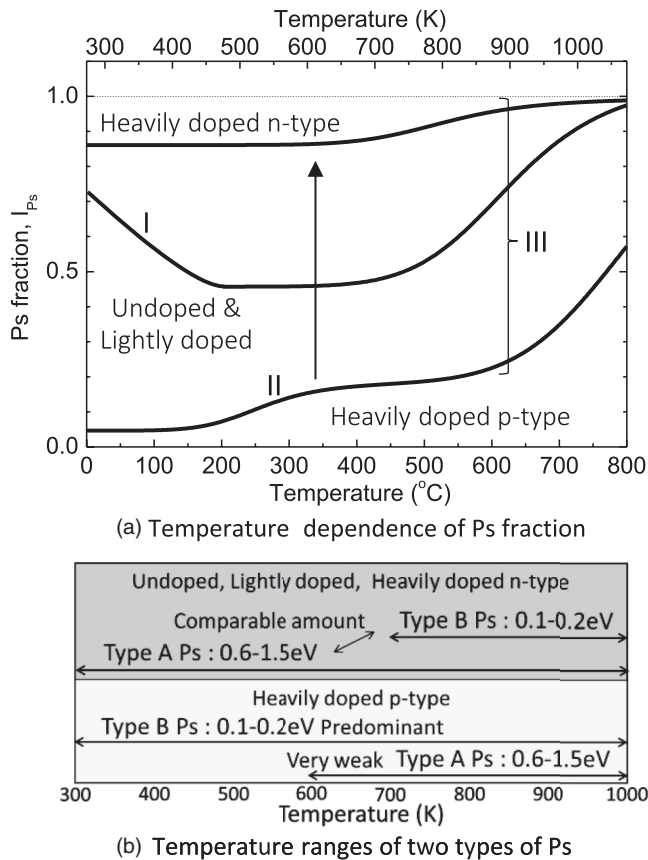
FIG. 5. Schematic representations of (a) temperature dependence of positronium fraction for the three typical doping conditions shown in Fig. 1, and (b) temperature ranges of type A and type B positronium distinguished by their energies.

A. Origins of the observed features: Type A positronium

In undoped and lightly doped Si and heavily doped n-type Si, type A positronium ($E_{Ps} = 0.6$–1.5 eV) exists in the whole temperature range, and hence it is likely to be formed via the work-function mechanism. The work function may be given by the threshold energy in the time-of-flight spectrum (i.e., $\Phi_{Ps}^{expt} = -1.5$ eV) rather than the peak energy of 0.6 eV. This is somewhat larger than the theoretical work function shown in Table II ($\Phi_{Ps}^{calc} = -0.42$ eV). Ordinarily, valance electrons are thought to take part in positronium formation. The theoretical positronium work function is indeed obtained using valence electrons. Assuming that conduction electrons are the source of the positronium, due to an additional energy gain of the band gap of Si, 1.1 eV, the theoretical work function would be $\Phi_{Ps}^{calc} = -0.42 - 1.1 \approx -1.5$ eV which agrees with the experimental value.

Actually, heavily doped n-type Si contains enough conduction electrons. In addition, as discussed for Fig. 3, the electric field due to the band bending effect promotes positrons to the surface as shown in Fig. 6(a). The high positronium yield can also be explained from this aspect. Since near the surface of heavily doped n-type Si, the depletion layer will be formed, the combination of positrons and conduction electrons may be suppressed there. Probably, conduction electrons outside the depletion region participate in type A positronium formation.
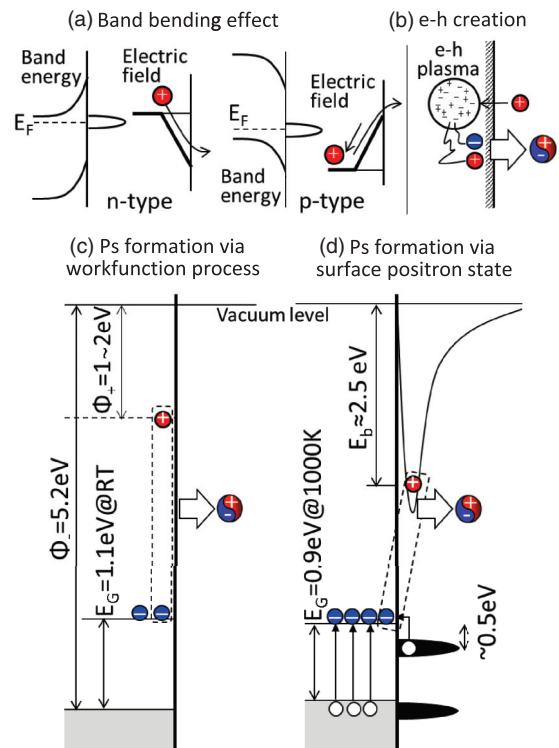
FIG. 6. Schematic representations of (a) band bending effect on positrons, (b) electron-hole plasma created by positron impact and resultant positronium formation, (c) positronium formation via work function mechanism, and (d) positronium formation via surface positron state.

The suppressed type A positronium formation in heavily doped p-type Si is explained as being due to the lack of conduction electrons. The repulsive surface potential to positrons may also reduce the type A positronium formation.

Since undoped and lightly doped Si are also deficient in conduction electrons, positronium formation from positrons and conduction electrons seems to be unlikely at first glance. As for this, the excitation of electron-hole (e-h) pairs by the impact of positrons should be considered, as shown in Fig. 6(b) [11]. In the present experiments ($E_+ = 200$ eV), approximately 50 e-h pairs will be created per positron in a sphere with a radius of about 10 Å. That is, the local e-h plasma density is 5×10^{21} cm^{-3}. Positronium formation may be possible between positrons and conduction electrons eluded from the e-h recombination.

The e-h plasma process seems to be more important in undoped and lightly doped Si, since the recombination lifetime of e-h pairs is very long (typically in the milliseconds) when the doping level is low. Furthermore, the carrier lifetime becomes shorter at elevated temperatures since the carrier capture cross section by gap states normally obeys the Arrhenius law. This may explain the decrease in the positronium fraction from 300 to 500 K in undoped and lightly doped Si [process I in Fig. 5(a)].

In heavily doped n-type Si, the conduction electrons excited by positron impact will decay rapidly through the capture process via impurity levels and also the drift into the deeper region by the band bending effect. Hence, the e-h excitation creates no significant effects in the temperature dependence. In

heavily doped *p*-type Si, the excited conduction electrons are also relaxed rapidly due to impurity levels and also via the drift to the surface by the band bending. Conversely, positrons will be repelled from the surface. Hence, positronium formation from positrons and conduction electrons will be rare at least at low temperatures. The small increase in the positronium fraction at 500–600 K [process II in Fig. 5(a)] may be partly explained as the thermal activation of positrons beyond the surface potential barrier and the combination with the excited conduction electrons [Fig. 6(a)].

Thus, type A positronium may be formed between positrons and conduction electrons via the work-function mechanism. Using the experimental positronium work function ($\Phi_{Ps}^{expt} = -1.5$ eV), the positron work function is estimated to be $\phi_+ = \Phi_{Ps} - \phi_- + 6.8 = -1.5 - (5.2 - 1.1) + 6.8 = +1.2$ eV. This estimate is a bit smaller than the present calculation listed in Table II ($\phi^{calc} = +1.8$ eV). Anyway, the positron work function should be positive in Si. This may have an important meaning in the detailed positronium formation process, as discussed in Sec. IV D below.

B. Origins of the observed features: Type B positronium

Type B positronium ($E_{Ps} = 0.1$–0.2 eV) is seen for all the doping conditions and is independent of surface orientation. The increase of positronium fraction above 700 K [process III in Fig. 5(a)] is caused by type B positronium. Above 700 K, electrons are thermally excited from the valence band to the conduction band. In the surface depletion layer, the Fermi level is relatively deeper than in the bulk region even for heavily doped Si [32]. Hence, the temperature dependence of conduction electron density may be locally and temporally similar for all doping conditions giving rise to similar temperature dependence of process III. Thus, "athermal" type B positronium may be formed from surface positrons and thermally excited conduction electrons. Indeed, the surface positron binding energy estimated as $E_B = E_S - \phi_- + 6.8 = -(0.1 \sim 0.2) - (5.2 - 1.1) + 6.8 = +2.5 \sim 2.6$ eV is comparable to the calculation listed in Table II.

In heavily doped *p*-type Si, type B positronium is also seen at low temperatures. Probably, the conduction electrons excited by positron impact drift to the surface region due to the band bending effect and combine with residual surface positrons, though positrons tend to be repelled from the surface. The small increase in the positronium fraction at 500–600 K [process II in Fig. 5(a)] may partly be explained as the increase in the surface positrons resulting from the thermal activation of positrons beyond the surface barrier. In the other types of Si, such a drift of conduction electrons to the surface is not strong enough to give rise to type B positronium formation at low temperatures. This is plausible for heavily doped *n*-type Si in which the conduction electrons excited by positron impact are repelled from the surface.

C. Temperature dependence

A monotonic temperature variation of the positronium fraction may be described as a competition of two processes, one of which is the thermal process. The positronium fraction is generally given as

$$I_{Ps}(T) = \frac{g(T)\Delta I}{r + g(T)}, \quad (4)$$

where ΔI is the maximum change of positronium fraction in the process, r and $g(T)$ represent the rates of the nonthermal and thermal processes, respectively, and T is temperature. For instance, in the thermal desorption of positronium observed for metal surfaces, $r = \lambda_S$, which is the annihilation rate of surface positrons, and $g(T) = (4kT/h) \exp[-E_S/(kT)]$, where k is the Boltzmann constant, h is the Planck constant, and $E_S = \phi_- + E_B - 6.8 eV \geqslant 0$ [33]. The three processes, I, II, and III, are described as follows.

Process I: The positronium formation rate is assumed to be proportional to the density of surviving conduction electrons at a certain time after the creation of an *e*-h plasma by positron impact and trapping by gap states. The competitive process may be other events, such as free positron annihilation. The excess electron density may be given as $n \propto \exp(-kt)$ and hence $g(T) \propto \exp(-kt)$, where t is time and k is the trapping rate of electrons into gap states. The trapping rate is $k = N_t v \sigma_t$, where N_t is the electron trap density, $v = (3kT/m_e)^{1/2}$ is the thermal velocity of conduction electrons with effective mass m_e, and σ_t is the cross section for capture of electrons by the traps. This cross section is generally given in the form of $\sigma_t \propto T^{-2} \exp[-\Delta E_I/(kT)]$, where ΔE_I is the energy difference between the bottom of the conduction band and the crossing point of the adiabatic potentials for the conduction band and the trap [34–36]. Hence $k \propto T^{-3/2} \exp[-\Delta E_I/(kT)]$. Thus, using Eq. (4), process I is described as

$$I_{Ps}^{I}(T) = \frac{\Delta I_I}{1 + A_{I1} \exp\{A_{I2} T^{-3/2} \exp[-\Delta E_I/(kT)]\}}, \quad (5)$$

where A_{I1} and A_{I2} are constants.

Process II: The positronium formation rate is dominated by the thermal activation of positrons to overcome the surface potential barrier. The available electron density is assumed to be independent of temperature. Hence, $g(T) \propto \exp[-\Delta E_{II}/(kT)]$, where ΔE_{II} is surface potential barrier. The competitive process may be the free positron annihilation rate. Thus, process II is described as

$$I_{Ps}^{II}(T) = \frac{\Delta I_{II}}{1 + A_{II} \exp[\Delta E_{II}/(kT)]}, \quad (6)$$

where A_{II} is a constant.

Process III: The annihilation of surface positrons and positronium formation from surface positrons and conduction electrons that are thermally excited from the valence band compete each other. Hence, $r = \lambda_S$ and $g(T) \propto n$. As discussed in Sec. IV B, because of the depletion layers, the temperature dependence of n for undoped Si may be a good approximation for all doping conditions. Thus, $g(T) \propto (N_v N_c)^{1/2} exp[-E_{gap}(T)/(2kT)]$, where N_v and N_c are the density of states of the top of the valence band and the bottom of the conduction band, respectively: $N_{v(c)} = 2(2\pi m_{h(e)}kT/h^2)^{3/2}$ with the effective hole (electron) mass, $m_{h(e)}$, and the temperature dependent band gap $E_{gap}(T) = 1.166 - 4.73 \times 10^{-4} T^2/(T + 636)$ [37]. Thus,

using Eq. (4),

$$I_{\text{Ps}}^{\text{III}} = \frac{\Delta I_{\text{III}}}{1 + A_{\text{III}} T^{-3/2} \exp[E_{\text{gap}}(T)/(2kT)]}, \quad (7)$$

where A_{III} is a constant.

The temperature dependences of heavily doped n-type Si, undoped and lightly doped Si, and heavily doped p-type Si were fitted using Eq. (7) with a constant term, Eqs. (5) and (7), and Eqs. (6) and (7) with a constant term, respectively. The solid lines in Fig. 2 are the obtained fitting curves. The observed temperature dependences are well described using the concepts described above. The potential barriers were estimated to be $\Delta E_{\text{I}} = 90\text{--}110$ meV and $\Delta E_{\text{II}} = 0.28\text{--}0.54$ eV. The former value may be reasonable as a nonradiative process [38]. From the latter value, the width of the depletion layer (= $[2\epsilon \Delta E_{\text{II}}/(eN_A)]^{1/2}$, where ϵ is the dielectric constant, e is the elementary charge and N_A is the acceptor concentration) is further estimated to be a few tens of nm [32].

D. Excitonic positronium formation

As discussed so far, positronium formation in Si may occur between positrons and conduction electrons via the work-function mechanism (type A) and between surface positrons and conduction electrons via the athermal process (type B).

The positivity of the positron work function gives further insight into the work-function mechanism. If the positron work function is negative, positronium may be formed in two ways: either a positron is emitted into the vacuum and then an electron hops onto the positron, or a quasipositronium state formed in the low electron density region is eventually emitted as a positronium. In the case of positive positron work function, the former process is prohibited. In Si, therefore, quasipositronium (excitonic electron-positron bound state) should be formed in the bulk subsurface region and these then transit to positronium in vacuum. More apparent emission of positronium generated in the bulk to the vacuum is known to occur in insulators [39]. In Si, the excitonic bound state probably has a large Bohr radius and low binding energy ($\sim$30 meV) and hence it will be invisible as positronium [40]. Since the excitonic bound state will be easily broken up by a phonon attack, the transition to the vacuum positronium occurs in a sufficiently short time.

Strictly to say, in the previous arguments of the type A positronium work function, the binding energy of the excitonic state should be considered. But, since it is rather low, its omission makes no seriously wrong estimations.

Athermal excitonic positronium formation at Si surfaces was originally proposed by the UCR group. The excitonic state was assumed to be formed between surface positrons and electrons in surface dangling-bond states by analogy with the surface excitons observed by time-resolved photoluminescence measurements. If surface electrons participate in the positronium formation, the temperature dependence may be different for different surface orientations. Also, since in heavily doped n-type Si the upper surface bands should be fully occupied, thus prohibiting electron excitation from the lower band, the positronium fraction may be independent of temperature. These are not consistent with the present observations shown in Fig. 2. Therefore, it is proposed that the athermal positronium is formed between surface positrons and mainly bulk conduction electrons. This may also be a form of excitonic positronium formation.

V. CONCLUSION

The temperature dependence of the positronium fraction at Si surfaces is rich in variety and depends on the doping condition. The diversity arises from two kinds of positronium that are produced via the work function and surface positron-mediated mechanisms. In both cases, an excitonic state may be formed between positrons and conduction electrons as a precursor of the final positronium state.

ACKNOWLEDGMENT

[1] S. Mohorovičić, Astron. Nachr. **253**, 93 (1934).

[2] M. Deutsch, Phys. Rev. **82**, 455 (1951).

[3] A. Rubbia, Int. J. Mod. Phys. A **19**, 3961 (2004).

[4] S. G. Karshenboim, Phys. Rep. **422**, 1 (2005).

[5] K. Shu, T. Murayoshi, X. Fan, A. Ishida, T. Yamazaki, T. Namba, S. Asai, K. Yoshioka, M. Kuwata-Gonokami, N. Oshima, B. E. O'Rourke, and R. Suzuki, J. Phys. Conf. Ser. **791**, 012007 (2017).

[6] M. Charlton and J. W. Humberston, *Positron Physics* (Cambridge University, New York, 2001).

[7] A. Ishii, Solid State Phenom. **28-29**, 213 (1992).

[8] A. P. Mills, Jr., in *Positron Spectroscopy of Solids*, edited by A. Dupasquire and A. P. Mills, Jr. (IOS, Amsterdam, 1993), p. 209.

[9] A. P. Mills, Jr., Phys. Rev. Lett. **41**, 1828 (1978).

[10] A. P. Mills, Jr., Solid State Commun. **31**, 623 (1979).

[11] D. B. Cassidy, T. H. Hisakado, H. W. K. Tom, and A. P. Mills, Jr., Phys. Rev. Lett. **106**, 133401 (2011).

[12] D. B. Cassidy, T. H. Hisakado, H. W. K. Tom, and A. P. Mills, Jr., Phys. Rev. Lett. **107**, 033401 (2011).

[13] D. B. Cassidy, T. H. Hisakado, H. W. K. Tom, and A. P. Mills, Jr., Phys. Rev. B **84**, 195312 (2011).

[14] D. B. Cassidy, T. H. Hisakado, H. W. K. Tom, and A. P. Mills, Jr., Phys. Rev. B **86**, 155303 (2012).

[15] S. Marder, V. W. Hughes, C. S. Wu, and W. Bennett, Phys. Rev. **103**, 1258 (1956).

[16] K. G. Lynn and D. O. Welch, Phys. Rev. B **22**, 99 (1980).

[17] P. G. Coleman, Solid State Phenom. **28-29**, 179 (1992).

[18] K. Wada, T. Hyodo, A. Yagishita, M. Ikeda, S. Ohsawa, T. Shidara, K. Michishio, T. Tachibana, Y. Nagashima, Y. Fukaya, M. Maekawa, and A. Kawasuso, Eur. Phys. J. D **66**, 37 (2012).

[19] A. Vehanen, K. Saarinen, P. Hautojärvi, and H. Huomo, Phys. Rev. B **35**, 4606 (1987).

[20] D. T. Britton, P. Willutzki, W. Triftshäuser, E. Hammerl, W. Hansch, and I. Eisele, Appl. Phys. A **58**, 389 (1994).

[21] J. A. Duffy, W. Bauer-Kugelmann, G. Kögel, and W. Triftshäuser, Appl. Surf. Sci. **116**, 241 (1997).

[22] X. Gonze, J.-M. Beuken, R. Caracas, F. Detraux, M. Fuchs, G.-M. Rignanese, L. Sindic, M. Verstraete, G. Zerah, F. Jollet, M. Torrent, A. Roy, M. Mikami, Ph. Ghosez, J.-Y. Raty, and D. C. Allan, Comput. Mater. Sci. **25**, 478 (2002).

[23] P. E. Blöchl, Phys. Rev. B **50**, 17953 (1994).

[24] J. P. Perdew, K. Burke, and M. Ernzerhof, Phys. Rev. Lett. **77**, 3865 (1996).

[25] B. Barbiellini, M. J. Puska, T. Torsti, and R. M. Nieminen, Phys. Rev. B **51**, 7341(R) (1995).

[26] R. M. Nieminen and M. J. Puska, Phys. Rev. Lett. **50**, 281 (1983).

[27] S. Hagiwara, C. Hu, and K. Watanabe, Phys. Rev. B **91**, 115409 (2015).

[28] V. Callewaert, K. Shastry, R. Saniz, I. Makkonen, B. Barbiellini, B. A. Assaf, D. Heiman, J. S. Moodera, B. Partoens, A. Bansil, and A. H. Weiss, Phys. Rev. B **94**, 115411 (2016).

[29] N. G. Fazleev, J. L. Fry, and A. H. Weiss, Phys. Rev. B **70**, 165309 (2004).

[30] S. Hagiwara, Y. Suzuki, and K. Watanabe, Defect Diffus. Forum **373**, 46 (2017).

[31] J. Kuriplach and B. Barbiellini, Phys. Rev. B **89**, 155111 (2014).

[32] S. M. Sze and K. K. Ng, *Physics of Semiconductor Devices*, 3rd ed. (Wiley, New York, 2007).

[33] S. Chu, A. P. Mills, Jr., and C. A. Murray, Phys. Rev. B **23**, 2060 (1981).

[34] C. H. Henry and D. V. Lang, Phys. Rev. B **15**, 989 (1977).

[35] H. Sumi, Phys. Rev. B **27**, 2374 (1983).

[36] Y. Kayanuma and S. Fukuchi, J. Phys. Soc. Jpn. **53**, 1869 (1984).

[37] J. S. Blakemore, *Semiconductor Statistics* (Dover, New York, 1987).

[38] K. W. Böer, *Survey of Semiconductor Physics* (Van Nostrand Reinhold, New York, 1990).

[39] Y. Nagashima, Y. Morinaka, T. Kurihara, Y. Nagai, T. Hyodo, T. Shidara, and K. Nakahara, Phys. Rev. B **58**, 12676 (1998).

[40] A. Dupasquier, in *Positron Solid-State Physics*, edited by W. Brandt and A. Dupasquier (North-Holland, Amsterdam, 1983), p. 510.